

Photonic Generation of Phase-Coded Millimeter-Wave Signal With Large Frequency Tunability Using a Polarization-Maintaining Fiber Bragg Grating

Ze Li, Ming Li, Hao Chi, Xianmin Zhang, and Jianping Yao, *Senior Member, IEEE*

Abstract—A photonic approach to generating a phase-coded millimeter-wave (mm-wave) signal with large frequency tunability is proposed and demonstrated. Two \pm second-order optical sidebands are generated by using a Mach-Zehnder modulator that is biased at the maximum transmission point and an optical notch filter. A polarization-maintaining fiber Bragg grating is then utilized to make the two sidebands orthogonally polarized. By sending the two orthogonally polarized sidebands to a polarization modulator, to which a phase-coding signal is applied, a frequency-quadrupled phase-coded mm-wave signal is generated. The generation of a phase-coded mm-wave signal with tunable frequencies at 40, 42, and 50 GHz is experimentally demonstrated. A pulse compression ratio of about 128 is achieved.

Index Terms—Microwave photonics, millimeter-wave signal generation, phase coding, pulse compression, radar.

I. INTRODUCTION

MICROWAVE pulse compression has been widely employed in modern radar systems to increase the range resolution [1]. Usually, microwave pulse compression is realized by compressing a frequency-chirped or phase-coded pulse using a matched filter. Although phase-coded pulses can be generated in the electrical domain, the time-bandwidth product (TBWP) is usually low, limited by the speed of the currently available digital electronics. An effective solution is to generate a phase-coded microwave pulse using photonic techniques [2]–[6]. In [2], [3], a phase-coded microwave pulse was generated based on optical pulse shaping using a spatial light modulator (SLM). The key advantage of using an SLM is the high flexibility. However, the fiber-to-space and space-to-fiber coupling would make the system complicated and lossy. A phase-coded microwave pulse can also be generated using pure fiber-optic components.

Manuscript received August 30, 2011; accepted September 27, 2011. Date of publication October 24, 2011; date of current version December 07, 2011. This work was supported by the Natural Sciences and Engineering Research Council of Canada (NSERC) and by a scholarship from the China Scholarship Council.

Z. Li is with the Microwave Photonics Research Laboratory, School of Electrical Engineering and Computer Science, University of Ottawa, Ottawa, ON K1N 6N5, Canada and also with the Department of Information Science and Electronic Engineering, Zhejiang University, Hangzhou 310027, China.

M. Li and J. Yao are the Microwave Photonics Research Laboratory, School of Electrical Engineering and Computer Science, University of Ottawa, Ottawa, ON K1N 6N5, Canada. (e-mail: jpyao@site.uOttawa.ca).

H. Chi and X. Zhang are with the Department of Information Science and Electronic Engineering, Zhejiang University, Hangzhou, 310027 China.

Color versions of one or more of the figures in this paper are available online at <http://ieeexplore.ieee.org>.

Digital Object Identifier 10.1109/LMWC.2011.2170673

In [4], [5], a phase-coded microwave pulse was generated by incorporating an optical phase modulator (PM) in one arm of a Mach-Zehnder interferometer [4] or in a Sagnac interferometer [5]. However, the systems in [4], [5] are sensitive to environmental variations due to the fact that the systems are interferometer-based. A phase-coded microwave pulse could also be generated based on a photonic microwave delay-line filter [6], in which the phase shift of a specific bit is achieved by an additional time delay to the specific tap. Since the phase shift is time-delay based which is frequency dependent, to ensure an accurate phase coding, the bandwidth of the generated signal should be narrow. In [7], a phase-coded millimeter-wave (mm-wave) pulse was generated using a polarization modulator (PolM), to which two orthogonally polarized light waves with a wavelength spacing corresponding to the generated mm-wave were applied. The major limitation of the approach is that the carrier frequency of the generated phase-coded mm-wave pulse is not tunable, since the orthogonality of the two light waves are achieved by passing the two parallelly polarized light waves through a polarization-maintaining fiber, which is dependent on the wavelength spacing.

In this letter, we propose and demonstrate a novel approach to generating a phase-coded mm-wave signal with a tunable frequency. In the proposed approach, a Mach-Zehnder modulator (MZM) that is biased at the maximum transmission point (MATP) is used to generate two \pm second-order optical sidebands plus the optical carrier. By using a fixed optical notch filter to filter out the optical carrier, two \pm second-order optical sidebands are generated. The two sidebands are then sent to a broadband polarization-maintaining fiber Bragg grating (PM-FBG) to make the two sidebands orthogonally polarized, and then sent to the optical input of a PolM. By applying a phase-coding signal to the PolM, the two sidebands are phase modulated. By beating the two sidebands at a photodetector (PD), a phase-coded frequency-quadrupled mm-wave signal is generated. Since the two sidebands are traveling in the same optical path, a stable operation is guaranteed. This scheme offers two additional advantages compared with the approach we reported in [7]. First, the orthogonality of the two light waves to the PolM is independent of the wavelength spacing, which allows the frequency of the phase-coded mm-wave signal to be continuously tunable with a large tunable range. Second, the generated signal is frequency quadrupled, which can ease the requirements for a high-frequency microwave drive signal and a wideband MZM as compared with the approaches reported in [5] and [7].

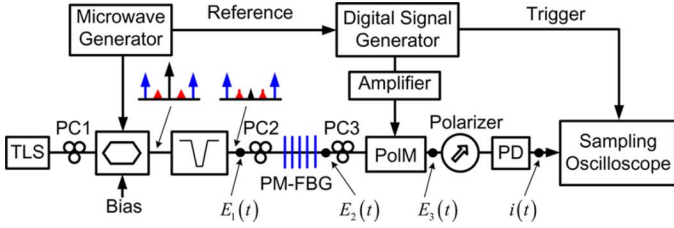


Fig. 1. Schematic of the proposed mm-wave phase-coding system.

II. PRINCIPLE

The schematic of the proposed mm-wave phase-coding system is shown in Fig. 1. A CW light wave from a tunable laser source (TLS) is sent to an MZM through a polarization controller (PC1). A sinusoidal microwave signal is applied to the MZM, which is biased at the MATP to generate two \pm second-order sidebands plus the optical carrier. The optical carrier is then suppressed by an optical notch filter. The two sidebands, with linear and identical polarizations, are then sent to a specially designed PM-FBG through a second PC (PC2), to adjust the incident angle at 45° relative to one principal axis of the polarization-maintaining fiber (PMF), in which the PM-FBG is written. Due to the birefringence in the PMF, the PM-FBG has two spectrally separated and orthogonally polarized transmission bands [8], [9]. The wavelength spacing between the two transmission bands is $\Delta\lambda = 2\Delta n_{\text{eff}}\Lambda$, where Δn_{eff} is the effective refractive index difference between the two orthogonal polarization states of the fundamental mode and Λ is the period of the grating. By aligning the two sidebands with the two transmission bands, two orthogonally polarized optical sidebands are obtained at the output of the PM-FBG. The two optical sidebands are then sent to the PolM through a third PC (PC3), with their polarization directions aligned with the two principal axes of the PolM. The PolM is a special phase modulator that has opposite modulation indices along the two principal axes [7], [10]. The two optical sidebands are complementarily phase-modulated within the PolM by a digital signal. By passing the two phase-modulated optical sidebands through a polarizer with its principal axis aligned at 45° relative to one principal axis of the PolM, and then beating the two sidebands at a PD, a phase-coded mm-wave signal with a frequency that is four times the frequency of the microwave drive signal is generated.

Mathematically, the optical signal at the output of the optical notch filter can be expressed as

$$\vec{E}_1(t) = A_{-2}e^{j(\omega_0 - 2\omega_m)t} + A_2e^{j(\omega_0 + 2\omega_m)t} \quad (1)$$

where ω_0 and ω_m are, respectively, the angular frequencies of the optical carrier and the microwave signal applied to the MZM, and A_{-2} and A_2 are the amplitudes of the two \pm second-order sidebands. The optical signal at the output of the PM-FBG is

$$\vec{E}_2(t) = \hat{x} \cdot A_{-2}e^{j(\omega_0 - 2\omega_m)t} + \hat{y} \cdot A_2e^{j(\omega_0 + 2\omega_m)t} \quad (2)$$

where \hat{x} and \hat{y} are the polarization directions corresponding to the principal axes of the PolM. If a binary digital signal $s(t)$ with the amplitude of V_p is applied to the PolM, the two sidebands at the output of the PolM can be expressed as

$$\vec{E}_3(t) = \hat{x} \cdot A_{-2}e^{j[(\omega_0 - 2\omega_m)t - \pi(V_p/V_\pi) \cdot s(t)]} + \hat{y} \cdot A_2e^{j[(\omega_0 + 2\omega_m)t + \pi(V_p/V_\pi) \cdot s(t)]} \quad (3)$$

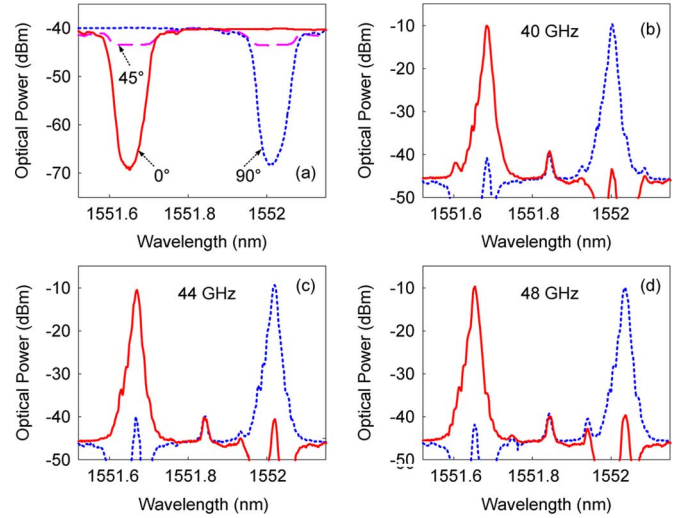


Fig. 2. (a) Transmission spectra of the PM-FBG measured using a broadband light source with its polarization direction aligned at an angle of 0° , 45° and 90° with respect to the fast axis of the PM-FBG. The optical spectra at the two outputs of the PBS for a microwave input signal at (b) 10 GHz, (c) 11 GHz, and (d) 12 GHz.

where V_π is the half-wave voltage of the PolM. Thus, the phase-coded mm-wave signal at the output of the PD is

$$i(t) = R \cdot A_2 A_{-2} \cos[4\omega_m t + 2\pi(V_p/V_\pi) \cdot s(t)] \quad (4)$$

where R is the responsivity of the PD. As can be seen from (4), a frequency-quadrupled phase-coded mm-wave signal is generated.

III. EXPERIMENTAL RESULTS AND DISCUSSION

The key component in the system is the PM-FBG, which is fabricated in a hydrogen-loaded PMF using a frequency-doubled argon-ion laser operating at 244 nm and a 15 cm long uniform phase mask. The spectra of the PM-FBG are measured using a broadband source, an optical linear polarizer and an optical spectrum analyzer (OSA). The polarizer is used to control the polarization state of the input light to the grating. Fig. 2(a) shows the transmission spectra of the PM-FBG measured when the polarization direction of the broadband light source is aligned at an angle of 0° , 45° and 90° with respect to the fast axis of the PM-FBG. The wavelength spacing between the two transmission bands is about 0.36 nm. Then, an experiment based on the setup shown in Fig. 1 is performed. The wavelength of the TLS is tuned to match the center of the two transmission bands of the PM-FBG. The power of the microwave signal from the signal generator (Agilent E8254A) is 25 dBm. A polarization beam splitter (PBS) is used to monitor the polarization states of the two sidebands at the output of the PM-FBG. Fig. 2(b)–(d) shows the optical spectra at the two outputs of the PBS when a microwave signal with its frequency at 10, 11, and 12 GHz applied to the MZM. As can be seen, a large isolation between the two optical sidebands of about 30 dB is achieved.

To demonstrate the phase-coding capability of the proposed system, a 42 GHz phase-coded signal is generated. The phase-coding signal is a 10.5 Gb/s “0101” digital sequence from a bit error rate tester (BERT), which is amplified before being applied to the PolM. The generated phase-coded signal is shown in

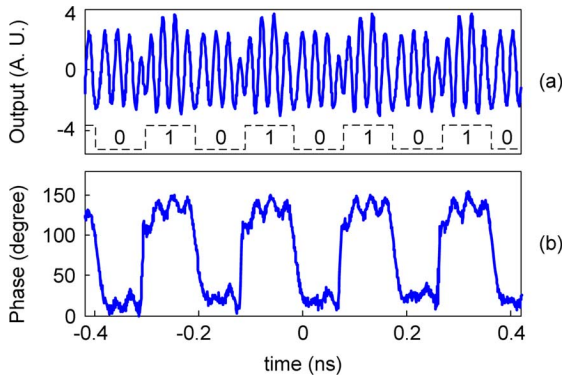


Fig. 3. (a) Generated 42 GHz phase-coded signal. (b) The recovered phase information from the phase-coded mm-wave signal in (a).

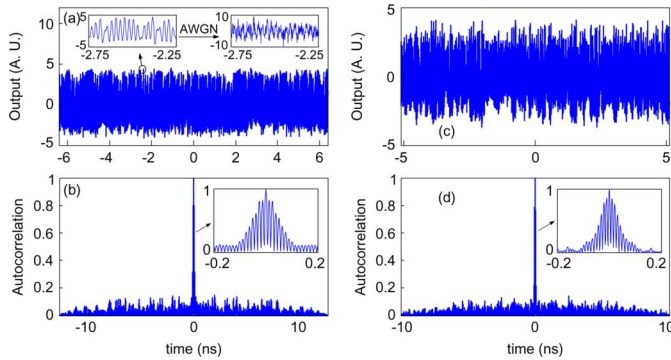


Fig. 4. Phase-coded signal and the calculated correlation between the original signal and the signal with an AWGN at different frequencies. (a)–(b) 40 GHz. (c)–(d) 50 GHz. Inset of (a): a section of the phase-coded signal without and with an AWGN. Insets of (b) and (d): zoom-in views of the peaks.

Fig. 3(a), which is monitored by a sampling oscilloscope (Agilent 86100C). Note that an average of 16 times is performed to remove the noise. In the experiment, the power P of the phase-coding signal at the output of the microwave amplifier is about 19 dBm. Thus, the amplitude V_p of the phase-coding signal is calculated to be 1.99 V based on $V_p = \sqrt{PZ_m}$ for a square wave, where the input impedance of the PoIM, Z_m , is 50 Ω . As the half-wave voltage of the PoIM is about 5 V, the phase shifts corresponding to bit “1” is calculated to be 143° according to (4). Fig. 3(b) shows the phase information of the phase-coded signal in Fig. 3(a) recovered using the Hilbert transform. As can be seen, the maximum phase shift is about 150° , which agrees well with the theoretical value.

To demonstrate the frequency tunability and the pulse compression capability, a phase-coded mm-wave signal at a new frequency of 40 GHz is generated. The phase-coding signal is a 10 Gb/s pseudo-random bit sequence (PRBS) with a length of 128 b. The power of the PRBS signal is increased to about 21 dBm to achieve a π phase shift, which can help improve the peak-to-sidelobe ratio (PSR) of the compressed pulse. Fig. 4(a) shows the generated 40 GHz phase-coded signal with a time duration of 12.8 ns. The TBWP is calculated to be 128. An additive white Gaussian noise (AWGN) is added to the generated signal to make the signal-to-noise ratio (SNR) as low as 0 dB, to show the robustness of the pulse compression. Fig. 4(b) shows the correlation between the original phase-coded signal (as a reference) and the phase-coded signal with an AWGN [5]. The autocorrelation peak has a full-width at half-maximum (FWHM) of about

0.102 ns, as shown in the inset of Fig. 4(b), corresponding to a compression ratio of about 125.2. Then, the frequency of the phase-coded signal is tuned to 50 GHz and the phase-coding signal is a 12.5 Gb/s 128 b PRBS. Fig. 4(c) shows the generated 50 GHz phase-coded signal with a time duration of 10.24 ns. Fig. 4(d) shows the correlation between the original 50 GHz phase-coded signal and the 50 GHz phase-coded signal with an AWGN. The compression ratio is about 131.1. The PSR in Fig. 4(b) and (d) is about 7, which is much larger than those in [5] and [7].

In the experiment, the minimum and maximum frequencies of the mm-wave signal are 40 and 50 GHz, which are restricted by the bandwidths of the PM-FBG. If a high birefringence PMF is used to fabricate the PM-FBG to have 0.6 nm wavelength spacing and a 0.3 nm bandwidth, the frequency tunable range can be increased from 40 to 110 GHz, which is sufficient for most of the applications. In the experiment, since the two sidebands are traveling in the same optical path, the stability of the system is excellent [7], which is much better than that of the system reported in [5].

IV. CONCLUSION

We have proposed and demonstrated a novel approach to generating phase-coded mm-wave signals with large frequency tunability. The key component in the system is the PM-FBG, which was employed to ensure the generation of two orthogonally polarized optical sidebands with tunable wavelength spacing. The phase coding was done in the PoIM and the beating of the two phase-modulated sidebands could generate an mm-wave phase-coded signal with a tunable frequency. The generation of a phase-coded signal with a tunable frequency at 40, 42, and 50 GHz was experimentally demonstrated. A pulse compression ratio of about 128 and a PSR of about 7 were achieved.

REFERENCES

- [1] M. I. Skolnik, *Introduction to Radar*. New York: McGraw-Hill, 1962.
- [2] J. D. McKinney, D. E. Leaird, and A. M. Weiner, “Millimeter-wave arbitrary waveform generation with a direct space-to-time pulse shaper,” *Opt. Lett.*, vol. 27, no. 5, pp. 1345–1347, Aug. 2002.
- [3] J. Chou, Y. Han, and B. Jalali, “Adaptive RF-photonics arbitrary waveform generator,” *IEEE Photon. Technol. Lett.*, vol. 15, no. 4, pp. 581–583, Apr. 2003.
- [4] H. Chi and J. P. Yao, “An approach to photonic generation of high-frequency phase-coded RF pulses,” *IEEE Photon. Technol. Lett.*, vol. 19, no. 10, pp. 768–770, May 2007.
- [5] Z. Li, W. Li, H. Chi, X. Zhang, and J. P. Yao, “Photonic generation of phase-coded microwave signal with large frequency tunability,” *IEEE Photon. Technol. Lett.*, vol. 23, no. 11, pp. 712–714, Jun. 2011.
- [6] Y. Dai and J. P. Yao, “Microwave pulse phase encoding using a photonic microwave delay-line filter,” *Opt. Lett.*, vol. 32, no. 24, pp. 3486–3488, Dec. 2007.
- [7] H. Chi and J. P. Yao, “Photonic generation of phase-coded millimeter-wave signal using a polarization modulator,” *IEEE Microw. Wireless Compon. Lett.*, vol. 18, no. 5, pp. 371–373, May 2008.
- [8] J. Hernandez-Cordero, V. A. Kozlov, A. L. G. Carter, and T. F. Morse, “Fiber laser polarization tuning using a Bragg grating in a Hi-Bi fiber,” *IEEE Photon. Technol. Lett.*, vol. 10, no. 7, pp. 941–943, Jul. 1998.
- [9] Y. Liu, K. S. Chiang, and P. L. Chu, “Generation of dual-wavelength picosecond pulses from a self-seeded Fabry-Perot laser diode and a polarization-maintaining fiber Bragg grating,” *IEEE Photon. Technol. Lett.*, vol. 16, no. 7, pp. 1742–1744, Jul. 2004.
- [10] J. D. Bull, N. A. F. Jaeger, H. Kato, M. Fairburn, A. Reid, and P. Ghanipour, “40 GHz electro-optic polarization modulator for fiber optic communications systems,” in *Proc. SPIE*, Dec. 2004, vol. 5577, pp. 133–143.